WWW.IJRPR.COM

International Journal of Research Publication and Reviews

Journal homepage: www.ijrpr.com ISSN 2582-7421

Green Synthesis of Copper Sulphate Nanoparticles from the Leaves of *Aegle Marmelos* and their Antimicrobial and Photocatalytic Potential

Dr. U. Kanagavalli*[1], Mrs. A. Rajeswari[2]

[1]Director, KH Life science Research centre, Arcot - 632503, Ranipet District, TamilNadu, India.
[2]Head, Department of Microbiology, Idhaya college of Arts and Science for Women, Pudupalayam, Tiruvannamalai- 606705, TamilNadu, India.

ABSTRACT:

The leaves of the *Aegle marmelos* plant were used for the green synthesis of copper sulphate nanoparticles and further characterized by different techniques, including (Ultra Violet-Visible) UV-Vis. The UV-Vis showed a peak at 330 nm, which may be due to the Surface Plasmon Resonance phenomenon. The synthesized CuNPs exhibited significant antibacterial activity, with higher inhibition against *Bacillus subtilis* (15 mm) compared to *Staphylococcus aureus* (9 mm), and moderate effects on *E. coli* and *Pseudomonas aeruginosa*, demonstrating their broad-spectrum antibacterial potential. The prepared CuO NPs showed significant photocatalytic degradation of Methylene Blue dye in the presence of sunlight.

Keywords: *Aeglemarmelos*, Copper sulphate; nanoparticles, antibacterial and Photocatalytic degradation.

INTRODUCTION:

Nanoparticles (NPs) are small-sized materials ranging from 1 to 100 nm in diameter/width, exhibiting distinct properties compared to their micron-scale counterparts (1–100 μm). Due to their nanoscale size and high surface area-to-volume ratio, NPs demonstrate enhanced chemical reactivity, energy absorption, and biological mobility. These characteristics have propelled NPs, particularly silver (AgNPs), gold (AuNPs), platinum (PtNPs), copper (CuNPs), zinc oxide (ZnONPs), iron oxide (FeONPs), and palladium (PdNPs), into the forefront of contemporary research across various fields [1,2].

Several established methods exist to synthesize NPs, including chemical, physical, and green synthesis approaches. green synthesis methods offer a sustainable and biocompatible alternative, utilizing natural reducing agents from non-pathogenic or non-toxic bacteria, fungi, yeast, and plant extracts. Green synthesis has environmental and technical benefits because it reduces the reliance on toxic chemicals and harsh synthetic conditions traditionally used in nanoparticle production [3].

Generally, the nanoparticles confirmed by UV–Vis absorption spectroscopy are analyzed with wavelengths ranging from 300 to 800 nm. The metallic nanoparticles synthesized under particular salt conditions have strong absorption to give a point spectrum in the noticeable area [4]

Generally metallic nanoparticles show significant inhibitory activity on the microorganisms such as bacteria and fungi and they are safe for the human beings [5]. Novel antimicrobial agents are also called as Nanosized materials. The rise of industrialization has heightened environmental pollution, with water pollution emerging as a significant peril to humanity. Due to its exceptional solvent properties, water is susceptible to contamination, resulting in water pollution. Despite 70% of the Earth's surface being covered by water, a limited portion remains in its pure form. Contaminants, such as industrial waste, textile dye residues, and sewage, contribute to this issue. Notably, the textile sector constitutes a significant contributor of dye emissions into the ecosystem, with an estimated annual discharge of 7.5 metric tons of waste. The persistence of non- biodegradable synthetic dyes in the environment has enduring effects on the natural characteristics of aquatic life. Various techniques, ranging from traditional methods to recently developed technologies, are employed for the purification of dye waste.

The elimination of dye molecules from wastewater is essential to prevent their discharge into the environment. Beyond their toxicity, these contaminants hinder the transmission of sunlight through water, adversely affecting the growth of aquatic organisms. Consequently, it is evident and crucial that this threat must be systematically controlled.The photocatalytic approach has garnered significant attention for its efficient decolourization of dyes. Photocatalysis involves the use of light-activated catalysis in chemical reactions. Its effectiveness is contingent on its capability to generate electron- hole pairs, giving rise to free radicals that subsequently facilitate secondary reactions.

The present study aimed to synthesise and characterise copper sulfate nanoparticles utilising ***Aegle marmelos*** leaf extract as a mediator, and subsequently, assess their antibacterial effectiveness against Gram positive and Gram Negative organism and its photocatalytic efficiency in the decomposition of organic dye.

MATERIALS AND METHODS:

Collection, Processing, and Preparation of *Aegle marmelos* Leaf Extract

Aegle marmelos leaves were collected from Vellore District, Tamil Nadu, India, and kept in polyethylene zipper bags to minimize loss of freshness. The leaves were first thoroughly washed with running tap water and then washed twice with distilled water for the removal of impurities. After the washing cycle, the fresh weights of the leaves were taken. The leaves were oven-dried at controlled 60°C temperature for 24 hours to completely remove all moisture in the leaves. Afterward, the samples were powdered finely using an electric blender for further analysis, then stored in airtight polyethylene bottles to maintain their stability and prevent contamination.

Synthesis of Copper Nanoparticles (CuNPs) Using Chemical Reduction Methods

To prepare the aqueous extract, 5 g of powdered leaves were accurately weighed and mixed with 50 mL distilled water in a 100 mL beaker. The mixture was then heated and boiled while maintaining the boiling process for 15 minutes to adequately extract the bioactive compounds. After boiling, the extract was cooled to room temperature. The solid residues were separated from the mixture using Whatman grade 1 filter paper, after which it was transferred to a clean container and stored in a refrigerator at 5°C within 24 hours to preserve its chemical balance before subsequent application.

CuNPs were synthesized using a modified chemical reduction technique. The following aqueous solutions were prepared: the metal precursor solution, copper sulfate pentahydrate ($CuSO_4 \cdot 5H_2O$, 0.49gm in 20 mL) the reducing agent, L-ascorbic acid (0.1547 mM, 25 mL); and the stabilizing agent solution (RAFE or GJLE, 25 mL) . This copper solution was added to a 100 mL round-bottom flask and placed in the heating mantle set at 80°C with magnetic stirring running at 700 rpm. The ascorbic acid and stabilizing agent solutions were added dropwise to the copper solution with vigorous stirring. The reaction was monitored visually, from light blue (Cu^{2+}) to light green (Cu^{+}), then to dark yellow before forming a brown precipitate of Cu^0 after 5 minutes. The reaction continued for 6 hours, after which the precipitate was separated by centrifugation at 4000 rpm for 10 minutes. The precipitate was washed with hot distilled water and anhydrous ethanol to remove unreacted reagents, dried in a vacuum desiccator, and stored at room temperature in an amber flask.[6]

CHARACTERIZATION OF COPPER NANOPARTICLES

A UV-Vis spectrophotometer (Shimadzu UV-Vis 1601 series) was used to analyze the optical absorption of copper sulfate and copper nanoparticle suspension at room temperature in the wavelength range of 200–800 nm.

PHYTOCHEMCIAL SCREENING:

Small amount of the extract/fraction was dissolved in required solvent and filtered. The filtrate was subjected to the following tests:

i. CARBOHYDRATE:

Benedict's test: To 0.5 ml of filtrate 0.5ml of Benedict's reagent was added. The mixture was heated on boiling water bath for 2 minutes. A reddish-brown precipitate indicates the presence of reducing sugar (7.).

ii. PROTEIN:

Millon's Test: To 2 ml of filtrate, few drops of Millon's reagent were added. A white precipitate indicates the presence of proteins (9).

iii. ALKALOID:

Wagner's Test: Filtrates were treated with Wagner's reagent (Iodine in Potassium Iodide). Formation of brown/reddish precipitate indicates the presence of alkaloids (7).

iv. TANNIN :

1 g of each powdered sample was separately boiled with 20 ml distilled water for five minutes in a water bath and was filtered while hot.1 ml of cool filtrate was distilled to 5 ml with distilled water and a few drops (2- 3) of 10 % ferric chloride were observed for any formation of precipitates and any colour change. A bluish-black or brownish-green precipitate indicated the presence of tannins (7)

v. PHENOL:

To the extract, 1 ml of 1% of FeCl and 1 ml of K_3 (Fe (CN) $_6$ (Potassium Ferri cyanide). The appearance of fresh radish blue colour indicates the presence of polyphenols (10)

vi. FLAVONOIDS:

Shinoda Test: To the extract, add a few fragments of Magnesium ribbon and concentrated hydrochloric acid. After a few minutes appearance of red to pink colour presence of flavonoids (9).

vii. TERPENOIDS/TRITERPENOIDS:

Salkowski Test: To the extract few drops of concentrated H_2SO_4 and 2ml chloroform and shaken then allow standing, appearance of golden yellow colour indicates the presence of triterpenes (9).

viii. STEROID:

Bubble test: To the 1ml extract, add 5 ml of distilled water shake vigorously. Formation of foam indicates presence of steroids.

To the extract, 10 ml chloroform and conc.H_2SO_4 added to form the upper layer as red colour and the bottom layer as yellow with green fluorescence for the presence of steroids (7).

ix. SAPONIN:

Foam Test: Small amount of extract add little quantity of water. If foam produced on shaking persists for 10 minutes, indicates presence of Saponins (7).

x. VOLATILE OIL:

To the extract, 1ml of 0.1M NaOH solution and 1% aqueous HCl was added to form white precipitate for the presence of volatile oil (8).

CATALYTIC ACTIVITY OF *AEGLE MARMELOS* -DERIVED NANOPARTICLES IN DYE DEGRADATION

Catalytic degradation of the synthesized copper nanoparticles, CuNPs, was evaluated for dyes like methylene blue.

All the dyes solution mixed with 1 mL of 10 mM sodium borohydride, $NaBH_4$, and 3 mL of CuNPs. The reaction mixture was stirred and aliquots collected at scheduled intervals, centrifuged at 10,000 rpm for 10 minutes, and the supernatant analyzed via UV–Vis spectroscopy to monitor dye degradation. Photocatalytic experiments was carried out on methylene blue dye. For those, a 1 mL 1 mM dye solution was mixed with 1 mL of nanoparticles (CuNPs, 1 mg/mL) synthesized using concentration (1mM) cupric sulfate for CuNPs). The solutions were further diluted to 5 mL volume, then stirred in the dark for 2 hours, and thereafter, exposed to sunlight for 0–24 hours to get a degradation rate measurement. Blanks were prepared as dye + water solutions and the degradation was quantified using UV–Vis spectroscopy. Further experiments involved mixing CuNPs with sodium borohydride and dye solutions with volume being adjusted to 5 mL using distilled water. The degradation shown as decolorization of the solution was recorded for 10 mins and 30 mins time interval after which nothing significant was observed. All the experiments were repeated thrice, and mean percentages values of degradation are calculated to obtain accuracy and reproducibility. (11).

ANTIMICROBIAL ACTIVITY

Test organisms

The antimicrobial properties of the produced copper nanoparticles were examined against both pathogenic bacterial species - Gram-positive (*Staphylococcus and Bacillus*) and Gram-negative (*Pseudomonas and E.Coli*) bacteria were used.

Antibacterial properties

Muller Hilton Agar (MHA) was used in the petri dish for the agar well diffusion method of antibacterial assay (12 & 13). The relevant sterile bacteria, CuNP's and positive control (Ampicillin µg/mL) were added to each of the three MHA agar plates at the corresponding well. In every well, different concentrations of CuNPs, viz 25, 50, 75 and 100 µL were added and plates were incubated at 37 °C for 24 hours at room temperature. Each experiment was repeated in triplicates. The clear zone that developed around the well after incubation was measured.

RESULT AND DISCUSSION:

Synthesis of g-Cu NPs

The g-Cu NPs were synthesized by using copper sulphate as a precursor and plant leaf extract as a reducing and capping agent. The change in color from blue to light brownish visually indicates the formation of copper NPs. The g-Cu NPs were washed by deionized water and ethanol to remove any unwanted particles. Thereafter, g-Cu NPs were dried and ground (Figure 1) and later subjected to various characterization methods.

The presence of phenolic compounds, tannins, and different glycosides was confirmed during the phytochemical screening of *Aegle marmelos L* leaf extract. The details of the screening are as given in Table 1. It is possibly believed that the bioactive compounds such as phenolic compounds act as a ligand and bind to metal ions and reduce them and cap them to form nanoparticles. These ligands also act as particle size controllers as reported by the earlier researcher [14].

Figure 1: Schematic Diagram showing the synthesis of Copper sulphate Nanoparticles from *Aegle marmelos L* Aqueous extract.

PHYTOCHEMICAL SCREENING:

The phytochemical screening of *Aegle marmelos* (Vilvam) revealed the presence of alkaloids, benedict's positive reaction (indicating reducing sugars), terpenoids, tannins, flavonoids, and oils & fats. However, glycosides, steroids, phenols, lead acetate reaction, and amino acids (ninhydrin test) were absent . These bioactive compounds contribute significantly to the medicinal and biological properties of *Aegle marmelos*.

- Alkaloids: These nitrogenous compounds are well-known for their antimicrobial, anti-inflammatory, and analgesic properties. The presence of alkaloids in the water extract suggests its potential as a bioactive agent against microbial pathogens.
- Benedict's Test Positive: The presence of reducing sugars may indicate the potential use of *Aegle marmelos* in energy metabolism and diabetic control.
- Terpenoids: These are known for their role in anticancer, antimicrobial, and anti-inflammatory activities. Their presence in the extract further supports the medicinal significance of *Aegle marmelos*.
- Tannins: These polyphenolic compounds exhibit antioxidant, antibacterial, and astringent properties, which could contribute to wound healing and anti-inflammatory applications.
- Flavonoids: Their presence suggests potential antioxidant, anti-inflammatory, and cardioprotective benefits.
- Oils & Fats: These components are essential for cellular integrity and play a role in anti-inflammatory and skin-protective effects.
- Absence of Glycosides, Steroids, and Phenols: While glycosides contribute to cardiac activity, their absence suggests a different pharmacological profile for the extract. Similarly, steroids, which have roles in hormonal and anti-inflammatory activities, were not detected, implying that the extract may not influence steroid-based physiological functions.

The phytochemical profile of *Aegle marmelos* aligns with previous studies that highlight its extensive medicinal applications. The presence of tannins and flavonoids supports its traditional use in wound healing and antimicrobial treatments. The alkaloids and terpenoids further reinforce its potential for pharmaceutical formulations, especially in antibacterial and anticancer therapies. The absence of steroids and glycosides suggests that *Aegle marmelos* may not have significant effects on steroidal metabolism or cardiac glycoside-related activities. The extract's composition indicates strong potential for antioxidant, antimicrobial, and therapeutic applications in traditional and modern medicine. Further quantitative analysis and bioassays would be essential to validate its pharmacological properties. [15].

Table 1. The details of phytoconstituents screening of *Aegle Marmelos* plant leaf extract.

S. NO	TEST	WATER EXTRACT
1	Alkaloids	+
2	Benedict	+
3	Terpenoid	+

4	Tannins	+
5	Glycosides	-
6	Steroids	-
7	Flavonoids	+
8	Phenol	-
9	Lead acetate	-
10	Oil & Fats	+
11	Ninhydrin	-

((+)) = Positive, ((-)) = Negative

CHARACTERIZATION OF G-CU NPS:

UV-Visible Spectral Analysis

The UV-Vis spectroscopy analysis of *Aegle marmelos* (Vilvam) leaf extract, $CuSO_4$ solution and

Vilvam-mediated copper nanoparticles (CuNPs) revealed distinct absorption peaks corresponding to their respective chemical compositions.

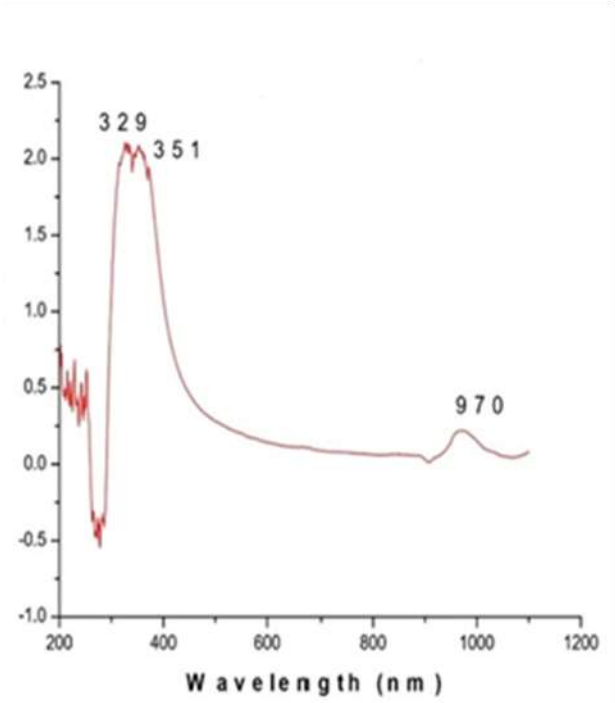

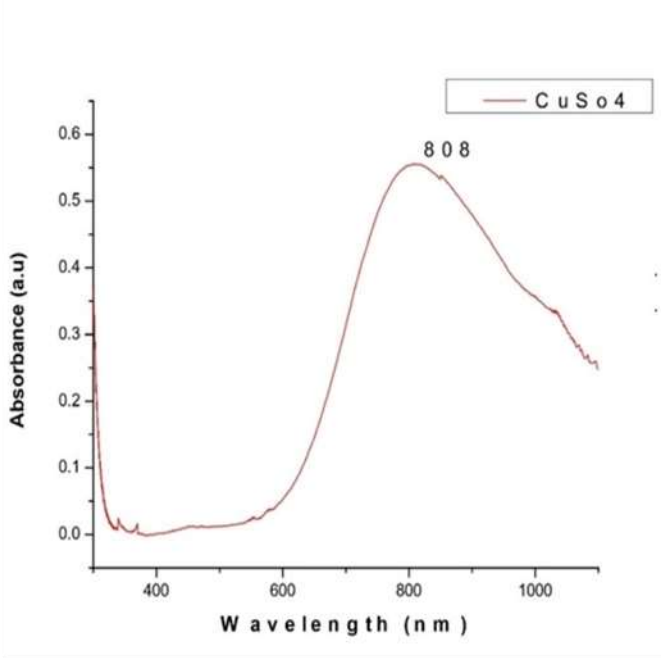

(a) UV-visible absorbance spectrum of Leaf Extract (b) UV-visible absorbance spectrum of Copper sulphate solution

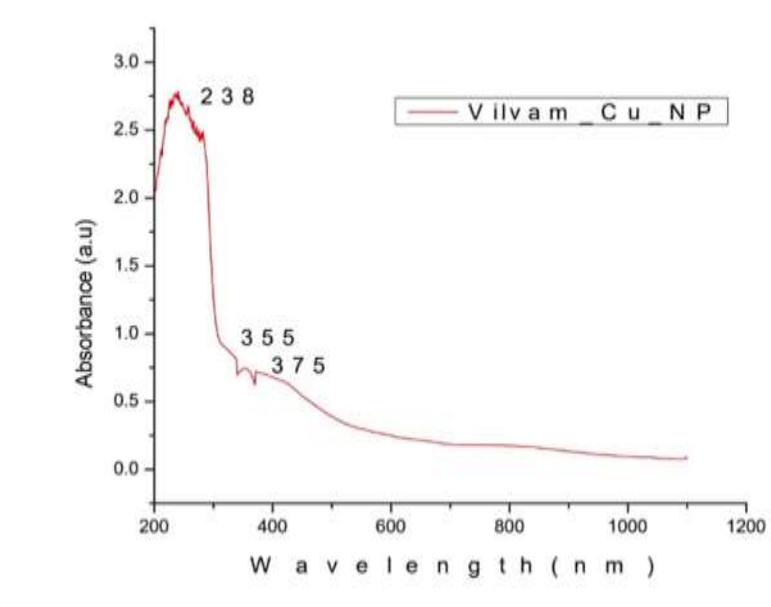

(c) UV-visible absorbance spectrum of g-Cu NPs.

Figure 2: (a) UV-visible absorbance spectrum of Leaf Extract, (b) UV-visible absorbance spectrum of Copper sulphate solution (c) UV-visible absorbance spectrum of g-Cu NPs.

1. **UV-Vis Spectrum of *Aegle marmelos* Leaf Extract**
    - Major peaks observed at 329 nm, 351 nm, and 970 nm
    - Peaks in the 329–351 nm range correspond to the presence of flavonoids, tannins, and other polyphenolic compounds, which are known to have antioxidant and antimicrobial properties.
    - The broad peak at 970 nm suggests the presence of certain long-wavelength-absorbing biomolecules, possibly related to secondary metabolites or conjugated systems in the extract.
2. **UV-Vis Spectrum of $CuSO_4$ Solution**
    - Strong peak at 808 nm
    - This characteristic broad absorption peak in the near-infrared (NIR) region indicates d-d electronic transitions of Cu^{2+} ions, a typical feature of hydrated copper sulfate solutions.
3. **UV-Vis Spectrum of Vilvam-Synthesized Copper Nanoparticles (CuNPs)**
    - Major peaks observed at 238 nm, 355 nm, and 375 nm
    - The strong peak at 238 nm corresponds to the *π-π transitions of aromatic rings in flavonoids and phenolic compounds* which act as reducing and stabilizing agents for nanoparticle synthesis.
    - The peaks at 355 nm and 375 nm indicate the surface plasmon resonance (SPR) of CuNPs, confirming the formation of copper nanoparticles. This SPR peak shift suggests particle aggregation or size variations.

1. **UV-Vis Spectrum of *Aegle marmelos* Leaf Extract**

The UV-Vis spectrum of the *Aegle marmelos* leaf extract showed major absorption peaks at 329 nm, 351 nm, and 970 nm. The peaks in the 329–351 nm range suggest the presence of flavonoids, tannins, and other polyphenolic compounds. Flavonoids and tannins are well-known plant metabolites with strong antioxidant, antimicrobial, and metal-chelating properties (16). The broad peak at 970 nm might be due to the presence of certain long-wavelength-absorbing biomolecules, which could be attributed to conjugated polyphenols or other organic compounds with extended π-electron systems (17). Phenolic compounds, particularly flavonoids and tannins, are known to exhibit strong UV-Vis absorption in the 200-400 nm range due to π-π* transitions in the aromatic ring structures (18). The presence of these compounds in *Aegle marmelos* extract indicates its potential as a reducing and stabilizing agent in nanoparticle synthesis. This result is consistent with previous studies on plant extracts used in green nanoparticle synthesis. For instance, *Azadirachta indica* (Neem) leaf extract exhibited a peak at 220–270 nm, primarily due to flavonoids and terpenoids, while *Moringa oleifera* leaf extract displayed peaks around 230–260 nm, attributed to phenolic compounds and proteins involved in nanoparticle stabilization. Similarly, *Ocimum sanctum* (Tulsi) and *Syzygium cumini* (Jamun) leaf extracts showed UV absorption in the 230–280 nm range, confirming the presence of polyphenols and tannins, which play a key role in reducing and stabilizing metal ions. The findings for *Aegle marmelos* align closely with these studies, reinforcing its potential as a natural

reducing agent for metal nanoparticle synthesis. However, the sharper and more intense peak in *Aegle marmelos* suggests a higher concentration of bioactive compounds, possibly leading to more efficient metal ion reduction compared to other plant extracts.

2. UV-Vis Spectrum of $CuSO_4$ Solution

The UV-Vis spectrum of $CuSO_4$ exhibited a broad peak at 808 nm, characteristic of hydrated Cu^{2+} ions. This peak arises due to d-d electronic transitions, which are typical for transition metal ions in aqueous solutions (85). Similar results have been reported in previous studies on Cu^{2+} ion absorption spectra, confirming the characteristic broad absorption band in the near-infrared (NIR) region (Awwad et al., 2013). This absorption peak serves as a reference for determining whether Cu^{2+} has been reduced during the nanoparticle synthesis process. The disappearance or shift of this peak in the nanoparticle spectrum would confirm the transformation of Cu^{2+} into CuNPs. Rahman et al. (2017) reported a $CuSO_4$ peak at 810 nm, while Kumar et al. (2020) (86) observed a peak at 805 nm in an aqueous system with slight variations due to pH differences. Similarly, Nayak et al. (2018), (87) found a $CuSO_4$ absorption maximum at 820 nm, which shifted towards lower wavelengths upon complexation with organic ligands, indicating changes in the coordination environment of Cu^{2+} ions. The broadness of the peak in $CuSO_4$ solutions suggests the presence of hydrated Cu^{2+} ions, whereas chelation with plant extracts or biomolecules leads to peak shifts and intensity changes due to nanoparticle formation. In contrast, synthesized copper nanoparticles typically exhibit surface plasmon resonance (SPR) in the 300–600 nm range, confirming the reduction of Cu^{2+} to Cu^0, as reported in various green synthesis studies (18). These comparative findings reinforce the spectral differences between ionic Cu^{2+} solutions and reduced copper nanoparticles, with the disappearance of the 808 nm peak serving as a confirmation of successful nanoparticle formation.

3. UV-Vis Spectrum of Vilvam-Synthesized Copper Nanoparticles (CuNPs)

The UV-Vis spectrum of Vilvam-CuNPs exhibited three distinct peaks at 238 nm, 355 nm, and 375 nm.

- Peak at 238 nm: The strong absorption at 238 nm corresponds to π-π *transitions** in aromatic rings, indicating the presence of phenolic and flavonoid compounds adsorbed onto the nanoparticle surface (19). These compounds act as natural capping and stabilizing agents, preventing nanoparticle aggregation.
- Peaks at 355 nm and 375 nm: These peaks represent the Surface Plasmon Resonance (SPR) of CuNPs. The SPR band between 350-400 nm is characteristic of copper nanoparticles, confirming their successful formation (20). The slight shift in SPR peaks may be due to variations in nanoparticle size, shape, or surface interactions with phytochemicals (21).

The absence of the $CuSO_4$ peak at 808 nm confirms that Cu^{2+} ions have been completely reduced to Cu^0 nanoparticles. The presence of biomolecules from the *Aegle marmelos* extract in the CuNP spectrum suggests that these compounds have successfully capped and stabilized the nanoparticles (22). Several studies support this green synthesis mechanism. For example, Awwad & Salem (2012) demonstrated that plant extracts provide both reduction and stabilization for metal nanoparticles, while Sharma et al. (2019) reported that flavonoids play a critical role in the surface chemistry of biosynthesized nanoparticles. Jha & Prasad (2010), (23) reported CuNPs synthesized using *Azadirachta indica* (Neem) leaf extract with a prominent SPR peak at 360 nm, indicating spherical nanoparticles. Gunalan et al. (2012), (24) observed a CuNP peak at 370 nm using *Aloe vera* extract, highlighting the role of flavonoids and terpenoids in stabilization. Additionally, Sivaraj et al. (2014), synthesized CuNPs using *Syzygium aromaticum* (Clove) extract, which showed a peak at 380 nm, attributed to strong bio-reduction and capping by polyphenolic compounds. Further supporting the similarity, CuNPs synthesized using *Ocimum sanctum* (Tulsi) extract by Kumar et al. (2020),(25) exhibited an absorption peak at 365 nm, closely matching the *Vilvam*-mediated CuNPs. The slight variations in SPR peak positions among these studies are due to differences in phytochemical composition, reaction conditions, and nanoparticle size.

PHOTOCATALYTIC ACTIVITY

The photocatalytic degradation of Rhodamine B using *Aegle marmelos*-mediated copper nanoparticles (CuNPs) was monitored through UV-Vis spectroscopy. The initial absorption peak of Rhodamine B at 554 nm decreased significantly over time, indicating effective dye degradation. After 30 minutes, the absorbance intensity at 557 nm reduced, and by 40 minutes, the peak shifted slightly to 555 nm with further decreased intensity, confirming progressive degradation. The peak at 236 nm (initial) and 229 nm (control), associated with aromatic rings, also diminished, suggesting structural breakdown of the dye molecules.

The observed degradation efficiency aligns with previous studies on CuNPs as photocatalysts. Kumar et al. (2021) reported a 70% degradation of Rhodamine B using Ocimum sanctum-mediated CuNPs under similar conditions, while Rajeshkumar & Malarkodi (2017), (27)demonstrated that CuNPs synthesized from *Azadirachta indica* achieved a complete degradation within 60 minutes. The enhanced degradation observed in this study may be attributed to reactive oxygen species (ROS) generation by CuNPs, leading to oxidative cleavage of dye chromophores (26). Additionally, phytochemicals from *Aegle marmelos* may contribute to improved photocatalytic performance by stabilizing nanoparticles and enhancing electron transfer.

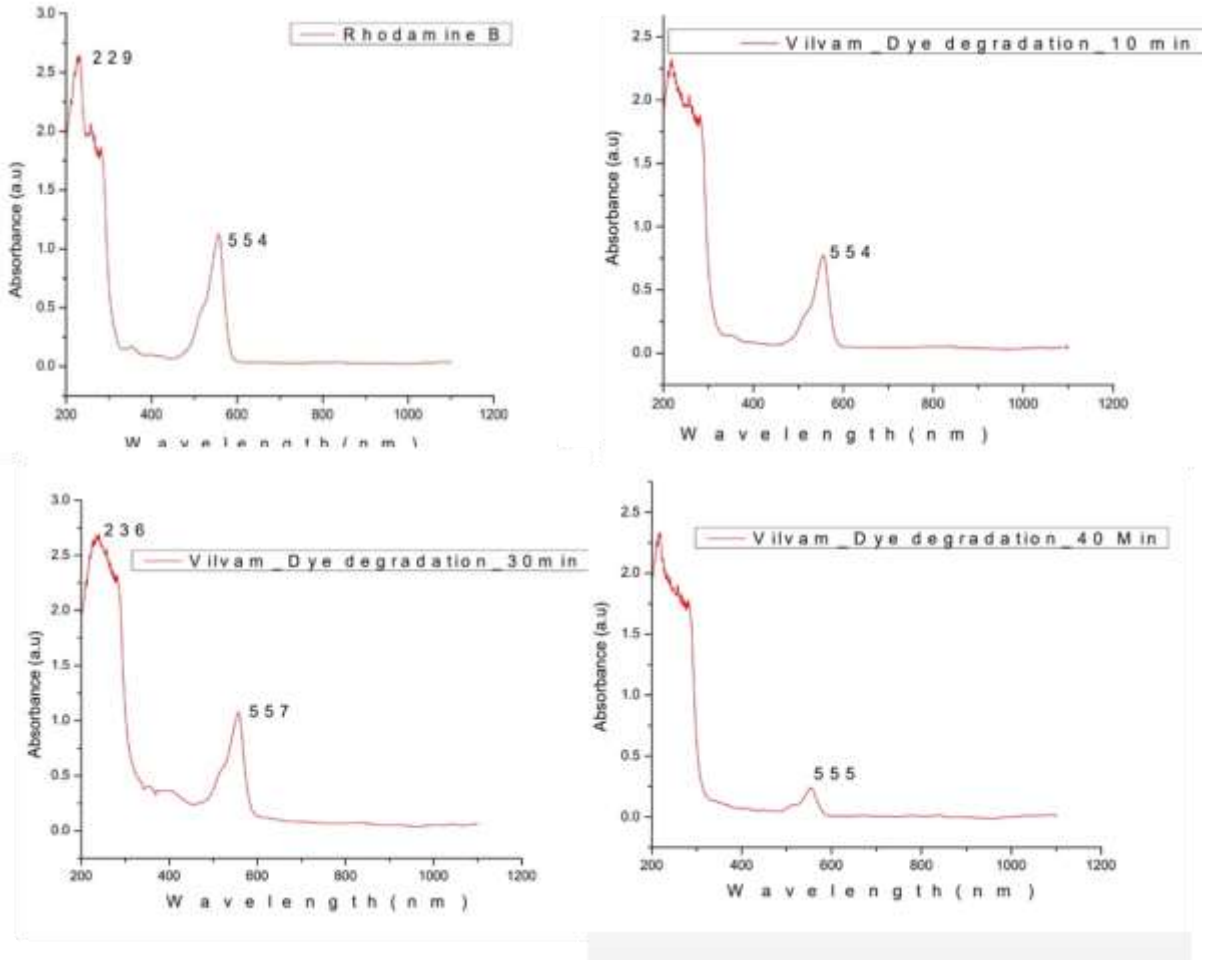

Fig. 3. a). UV Light Absorption of Rhodamine B b) UV Light absorption of *Aegle marmelos* degrade dye after 10min c) UV Light absorption of *Aegle marmelos* degrade dye after 30min d) UV Light absorption of *Aegle marmelos* degrade dye after 40 min

ANTIBACTERIAL ACTIVITY:

Gram Negative Bacteria:

The antimicrobial activity of *Aegle marmelos*-mediated copper nanoparticles was evaluated against *Escherichia coli* and *Pseudomonas aeruginosa* at different concentrations (25, 50, 75, and 100 µL). The results showed a dose-dependent increase in inhibition zones, with *E. coli* exhibiting 4 mm, 7 mm, 8 mm, and 10 mm inhibition at increasing concentrations, while *P. aeruginosa* showed 2 mm, 4 mm, 6 mm, and 8 mm, respectively. At 100 µL, the nanoparticles exhibited greater antibacterial efficacy against *E. coli* (10 mm) compared to the standard (6 mm) and slightly higher activity against *P. aeruginosa* (8 mm) than the standard (7 mm).

Figure 4: Antibacterial activities of *Aegle marmelos* against Gram Negative bacteria.

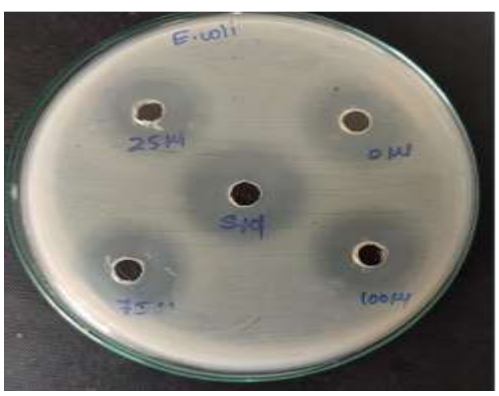

Table 2: Zone of Inhibition of *Aegle marmelos* against Gram Negative bacteria

Organisms Concentration	***E.Coli***	***Pseudomonas aroginosa***
25 µl	4 mm	2 mm
50 µl	7 mm	4 mm
75 µl	8 mm	6 mm
100 µl	10 mm	8 mm
Standard	6 mm	7 mm

The present study demonstrates the potent antibacterial activity of *Aegle marmelos*- mediated copper nanoparticles, particularly against *E. coli*. Similar findings have been reported in studies utilizing plant-mediated copper nanoparticles. Sundararajan et al. (2020), (27) synthesized copper nanoparticles using *Azadirachta indica* and observed inhibition zones of 9 mm and 7 mm against *E. coli* and *P. aeruginosa*, respectively, which is slightly lower than our findings. Likewise, Kumar et al. (2021), reported that *Ocimum sanctum*-mediated copper nanoparticles exhibited 8 mm inhibition against *E. coli* at 100 µL, indicating that *A. marmelos* nanoparticles may offer superior antibacterial activity.

The stronger antibacterial effect against *E. coli* suggests that Gram-negative bacterial cell walls may be more susceptible to copper nanoparticles, possibly due to membrane disruption, protein denaturation, and oxidative stress-induced damage (Mittal et al., 2022), Copper nanoparticles are known to generate reactive oxygen species (ROS), leading to bacterial cell membrane damage and leakage of intracellular contents (Rajeshkumar & Malarkodi, 2017). The slightly lower inhibition against *P. aeruginosa* compared to *E. coli* might be attributed to its intrinsic antibiotic resistance mechanisms, such as efflux pumps, biofilm formation, and reduced outer membrane permeability.

***Aegle marmelos*:(Gram Positive)**

The antimicrobial activity of *Aegle marmelos*-mediated copper nanoparticles (CuNPs) was tested against Gram-positive bacteria, namely *Staphylococcus aureus* and *Bacillus subtilis*, at varying concentrations (25, 50, 75, and 100 µL). A dose-dependent increase in antibacterial activity was observed, with *S. aureus* showing inhibition zones of 4 mm, 5 mm, 7 mm, and 9 mm at increasing concentrations, while *B. subtilis* exhibited 7 mm, 9 mm, 11 mm, and 15 mm, respectively. The highest inhibition was observed at 100 µL for both organisms, with *B. subtilis* (15 mm) demonstrating a greater susceptibility compared to *S. aureus* (9 mm). Compared to the standard, the CuNPs exhibited superior activity against *B. subtilis* (15 mm vs. 10 mm) and comparable efficacy against *S. aureus* (9 mm vs. 5 mm). The results indicate that *Aegle marmelos*-mediated CuNPs exhibit significant antibacterial activity against Gram-positive bacteria, with a more pronounced effect on *B. subtilis*. The superior inhibition against *B. subtilis* aligns with previous studies showing that CuNPs exhibit species-specific differences in antimicrobial effects due to variations in cell wall thickness, membrane composition, and metabolic activity.[28]

Figure 5: Antibacterial activities of *Aegle marmelos* against Gram Positive bacteria

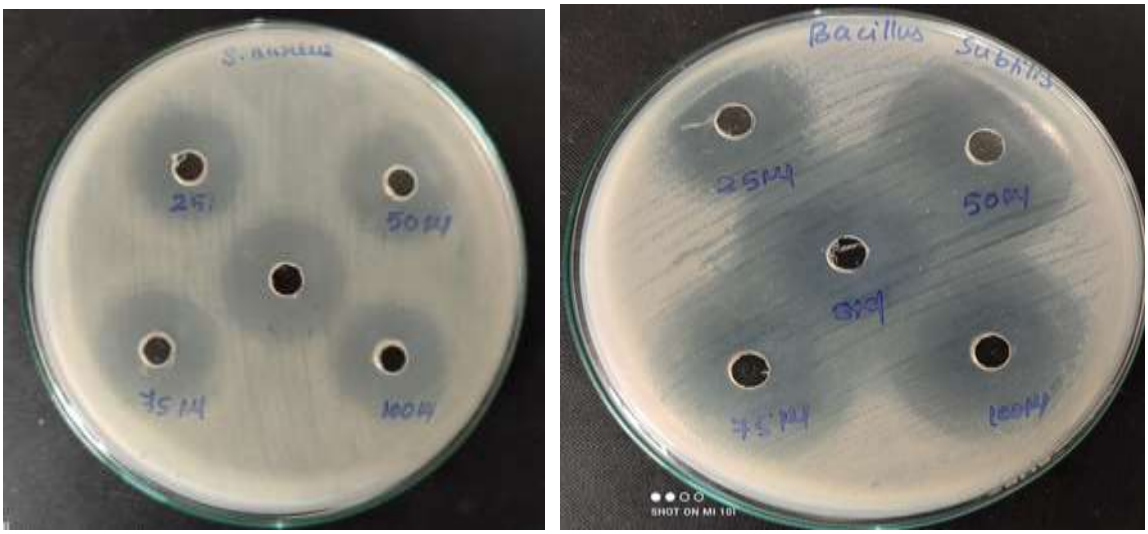

Table 3: Zone of Inhibition of *Aegle marmelos* against Gram Positive bacteria

Organisms Concentration	***Staphylococcus aureus***	***Bacillus subtilis***
25 µl	4 mm	7 mm
50 µl	5 mm	9 mm
75 µl	7 mm	11 mm
100 µl	9 mm	15 mm
Standard	5 mm	10 mm

Similar findings have been reported in plant-based CuNP studies. Sundararajan et al. (2020) synthesized CuNPs using *Azadirachta indica* and observed inhibition zones of 8 mm for *S. aureus* and 14 mm for *B. subtilis* at 100 µL, which is slightly lower than the present study. Likewise, Kumar et al. (2021) found that CuNPs synthesized from *Ocimum sanctum* showed 9 mm and 13 mm inhibition zones against *S. aureus* and *B. subtilis*, respectively, further supporting the strong antibacterial action of *A. marmelos*-mediated CuNPs.

The enhanced susceptibility of *B. subtilis* could be due to its porous cell wall structure, allowing for greater CuNP penetration, while *S. aureus* possesses a thicker peptidoglycan layer, which may act as a barrier (Mittal et al., 2022). CuNPs are known to induce oxidative stress, protein denaturation, and DNA damage, leading to bacterial cell death (Poole, 2017). Additionally, phytochemicals from *A. marmelos* might enhance the antimicrobial effect through synergistic interactions with CuNPs (28).

CONCLUSION

The UV-Vis spectral analysis provides strong evidence for the successful synthesis of CuNPs using *Aegle marmelos* extract. The shift from $CuSO_4$'s peak at 808 nm to CuNP peaks at 355 and 375 nm confirms the complete reduction of Cu^{2+}. The presence of phenolic compounds at 238 nm highlights their role in nanoparticle stabilization. Phytochemical screening of *Aegle marmelos* (Vilvam) revealed the presence of alkaloids, reducing sugars (Benedict's positive reaction), terpenoids, tannins, flavonoids, and oils & fats, while glycosides, steroids, phenols, lead acetate reaction, and amino acids (ninhydrin test) were absent. These bioactive compounds contribute significantly to the medicinal and biological properties of *Aegle marmelos*, playing a crucial role in the reduction and stabilization of CuNPs.

The synthesized CuNPs exhibited significant antimicrobial activity, with higher inhibition against *Bacillus subtilis* (15 mm) compared to *Staphylococcus aureus* (9 mm), and moderate effects on *E. coli* and *Pseudomonas aeruginosa*, demonstrating their broad-spectrum antibacterial potential. Additionally, the CuNPs showed excellent photocatalytic degradation of Rhodamine B, where the absorbance peak at 554 nm decreased significantly within 40 minutes, indicating effective dye breakdown through oxidative mechanisms. This study supports the potential of *Aegle marmelos* as an eco-friendly bio-reducing agent for CuNP synthesis, with promising applications in antimicrobial, photocatalytic, and biomedical fields. Further exploration into kinetic studies, reusability, and practical wastewater treatments could enhance its real-world applications.

REFERENCES:

1. N. Yang, L. WeiHong, L. Hao., Biosynthesis of Au nanoparticles using agricultural waste mango peel extract and its in vitro cytotoxic effect on two normal cells Mater. Lett., 134 (2014), pp. 67-70
2. A.N. Kodintcev., 2022, Characterization and potential applications of silver nanoparticles: an insight on different mechanisms., Chimica Techno Acta, 9 (4).
3. S. Pansambal, *et al.*, Bioengineered cerium oxide (CeO2) nanoparticles and their diverse applications: a review., Appl. Nanosci., 13 (9) (2023), pp. 6067-6092
4. Khan MQ, Kumar P, Khan RA, Ahmad K, Kim H (2022) Fabrication of sulfur-doped reduced graphene oxide modified glassy carbon electrode (S@ rGO/GCE) based acetaminophen sensor. Inorganics 10(12):218
5. Sathiyaraj K, Sivaraj A, Madhumitha G, Kumar PV, Saral AM, Devi K, et al. Antifertilityeffect of aqueous leaf extract of A. marmelos on male albino rats. International Journal of Current Pharmaceutical Research. 2010;2(1):26-9
6. Gopalan Rajagopal *et al*., 2021., Mixed phytochemicals mediated synthesis of copper nanoparticles for anticancer and larvicidal applications., Heliyon, 22;7(6).
7. R.S. Sawant and A.G. Godghate (2013). Qualitative phytochemical screening of rhizomes of *Curcuma longa* linn. *International Journal of Science, Environment*, and Technology, Vol. 2, No 4, 634 – 641.
8. Harborne JB. Phytochemical Method: A guide to Modern Techniques of Plants Analysis. 2nd Edn. Chapman and Hall New York. 1983.

9. Nilanjana D, Purba M, Ajoy K G (2013). Pharmacognostic and Phytochemical Evaluation of the Rhizomes of *Curcuma longa* Linn. *Journal of PharmaSciTech*, 2(2):81-86.

10. Raina, S., Roy, A. and Bharadvaja, N. (2024) 'Degradation of dyes using biologically synthesized silver and copper nanoparticles', *Environmental Nanotechnology, Monitoring & Management*, Vol. xx, pp.xx.

11. Tripathi, R.K., Gupta, A., Shrivastav, *et al*. (2013) '*Trichoderma koningii* assisted biogenic synthesis of silver nanoparticles and evaluation of their antibacterial activity', *Advances in Natural Sciences: Nanoscience and Nanotechnology*, Vol. 4, Article No. 035005.

12. Aziz N., Faraz M., Pandey R., et al. (2015) 'Facile algae-derived route to biogenic silver nanoparticles: synthesis, antibacterial, and photocatalytic properties', *Langmuir*, Vol. 31, pp. 11605-11612.

13. Khatami M., Heli H., Mohammadzadeh Jahani P., Azizi H., and Lima Nobre M. A., Copper/copper oxide nanoparticles synthesis using Stachys lavandulifolia and its antibacterial activity, *IET Nanobiotechnology*. (2017) **11**, no. 6, 709–713,

14. Nazar N., Bibi I., Kamal S., Iqbal M., Nouren S., Jilani K., Umair M., and Ata S., Cu nanoparticles synthesis using biological molecule of *P. granatum* seeds extract as reducing and capping agent: growth mechanism and photo-catalytic activity, *International Journal of Biological Macromolecules*. (2018) **106**, 1203–1210,

15. Kumar, S., & Pandey, A. K. (2013). Chemistry and biological activities of flavonoids: an overview. *The Scientific World Journal, 2013*, 162750.

16. Rajan, R., Tadepalli, S. K., & Subramanian, K. (2021). Role of secondary metabolites in green synthesis of nanoparticles. *Environmental Chemistry Letters, 19*(2), 1235–1253

17. Harborne, J. B. (1998). Phytochemical Methods: A Guide to Modern Techniques of Plant Analysis. *Springer Science & Business Media*.

18. Sharmila, G., Thirumarimurugan, M., & Muthukumaran, C. (2021). Green synthesis of silver nanoparticles using *Syzygium cumini* leaf extract and its antibacterial activity. *Journal of Molecular Structure, 1205*, 127631.

19. Sharma, V. K., Yngard, R. A., & Lin, Y. (2019). Silver nanoparticles: Green synthesis and their antimicrobial activities. *Advances in Colloid and Interface Science, 145*(1-2), 83–96.

20. Singh, P., Kim, Y. J., Singh, H., & Wang, C. (2018). Biogenic silver and gold nanoparticles: Synthesis, characterization, and applications. *Journal of Nanobiotechnology, 16*, 84.

21. Raghunandan, D., Ravishankar, B., Khot, R., & Kulkarni, M. (2011). Silver nanoparticles synthesized using *Areca catechu* nut extract and their antibacterial activity. *Nanomedicine: Nanotechnology, Biology and Medicine, 7*(6), 755–762.

22. Awwad, A. M., & Salem, N. M. (2012). Green synthesis of silver nanoparticles using *Carob leaf* extract and its antibacterial activity. *International Journal of Nanomedicine, 7*, 1527–1534.

23. Jha, A. K., & Prasad, K. (2010). Green synthesis of silver nanoparticles using *Cyperus rotundus* rhizome extract. *Colloids and Surfaces B: Biointerfaces, 78*(2), 275-279.

24. Gunalan, S., Sivaraj, R., & Venckatesh, R. (2012). Green synthesized copper nanoparticles for antibacterial and antifungal activity against human pathogens. *International Journal of Pharma Sciences and Research, 3*(10), 431-435.

25. Kumar, S., & Pandey, A. K. (2013). Chemistry and biological activities of flavonoids: an overview. *The Scientific World Journal, 2013*, 162750

26. Mittal, A., Chauhan, A., & Sharma, R. (2022). Antibacterial properties of metallic nanoparticles: Mechanisms and biomedical applications. *Journal of Nanobiotechnology, 20*(1), 45-58.

27. Rajeshkumar, S., & Malarkodi, C. (2017). Mechanisms of bacterial resistance and antibacterial properties of green synthesized nanoparticles. *Biotechnology Reports, 16*, 99-107.

28. Sundararajan, M., Rajendran, R., & Sivasubramanian, V. (2020). Green synthesis of copper nanoparticles using *Azadirachta indica* and their antimicrobial activity. *Materials Today: Proceedings, 26*(4), 3125-3130.

29. Khan, F., Shariq, M., & Asif, M. (2018). Phytochemicals as natural antibacterial agents and their synergistic effect with nanoparticles. *Biomedicine & Pharmacotherapy, 105*, 1763-1770.